Astron. Astrophys. 361, L9–L12 (2000)

ASTRONOMY AND ASTROPHYSICS

LETTER

Letter to the Editor

ADONIS observations of the HD 100546 circumstellar dust disk⋆

E. Pantin[1], **C. Waelkens**[2], **and P.O. Lagage**[1]

[1] DSM/DAPNIA/Service d'Astrophysique, CEA/Saclay, 91191 Gif-sur-Yvette, France
[2] Instituut voor Sterrenkunde, Celestijnenlaan 200B, 3001 Leuven, Belgium

Received 29 June 2000 / Accepted 15 July 2000

Abstract. We report in this letter the first resolved images of the circumstellar dust disk around the Pre-Main-Sequence star HD 100546. These near-infrared images were obtained in J and short K bands with the adaptive optics system ADONIS at the ESO observatory. A bright disk extending 2 arcsec (200 AU) far from the star and viewed with an inclination with respect to the line of sight around 50 degrees is revealed by the observations. Using a simplified model of light scattering, we find that the dust disk density peaks at a distance of 40 AU from the star, and the FWHM of this dense ring is typically 20 AU. This type of disk is believed to be a denser precursor of β Pictoris-like main-sequence disks. The structure of the disk is compared with the best known example of the class of "debris disks", the disk surrounding β Pictoris.

Key words: scattering – methods: data analysis – stars: binaries: eclipsing

1. Introduction

The discovery of infrared excesses around an important fraction of main-sequence stars (Aumann et al. 1984; Plets & Vynckier 1999) and attributed to the presence of cool dust grains orbiting the star and geometrically arranged in a disk, has triggered a lot of studies because these disks may be linked to planetary formation. For a long time the disk around the star β Pictoris was the only example to be resolved both in the visible (Smith & Terrile 1984) and in the mid-infrared range (Lagage & Pantin 1994). Recent discoveries of young "debris" circumstellar disks around relatively "old" and isolated (i.e. not associated to any star forming region) stars have shown that this phenomenon extends towards Pre-Main-Sequence stars (cf the photometric survey by Malfait et al. 1998a). The detection and resolution of disk around stars such as HD 141569 (Weinberger et al. 1999; Augereau et al. 1999) or HR 4796A thanks to high-resolution observations in the visible/near-infrared range (Schneider et al. 1999; Augereau et al. 1999) or mid-infrared images (Koerner et al. 1998; Jayawardhana et al. 1998) have shown the possibility to observe and study precursors to main-sequence dust disks. These so-called "baby-β Pic" dust disks are the denser precursors to main-sequence debris disks. IRAS and ISO/SWS observations have shown that they usually produce a huge infrared excess (typically 250 times the infrared excess produced by the β Pic disk); some of them, as HD 100546 for instance, showing prominent signatures of crystalline water ice (Waelkens et al. 1996, Malfait et al. 1998b), are particularly interesting targets in the visible/near-infrared because of high particle albedo. Observing this class of disks at various stages of evolution will help in finding a comprehensive scenario for the origin, the evolution, and the lifetime of the Vega phenomenon, i.e. how these disks form, how long they last, and how they disappear.

We report in this paper the first images of the disk around HD 100546, an isolated young main-sequence star. Using a model of scattering by dust grains, we derive the morphology of the disk outwards 10 AU and show evidence for a density maximum around 40 AU. The structure of the disk is compared to the best known example of the Vega Phenomenon, the disk around β Pic.

2. Observations

We observed the HD 100546 star (m_v=6.7) using the SHARP II+ camera coupled with the adaptative optics system ADONIS, and mounted on the ESO 3.6m telescope at La Silla, Chile. A pre-focal optics coronograph (Beuzit et al. 1997) was used to reject the direct starlight and increase the integration time in each elementary exposure. The mask size we used has a diameter of 0.74″. J (1.25 μm) and Ks (2.15 μm) band exposures were obtained on nights 23 and 24 of June, 1999. The seeing was quite variable the first night, but had decreased to a value of $0.7''$ at the time of the J and Ks observations. It was stable at a value around $0.85''$ during the second night. We spent a total observing time of 1550 s in the Ks band and 2600 s in the J band. The Point Spread Function (PSF) was frequently monitored thanks to interlaced observations of two reference stars, HD 97218 and HD 101713. These reference stars were used later in the reduction process to remove the wings of the stellar PSF and

Send offprint requests to: E. Pantin

⋆ based on observations collected on the ESO 3.6m telescope at La Silla, proposal 63.H-0239

Correspondence to: epantin@cea.fr

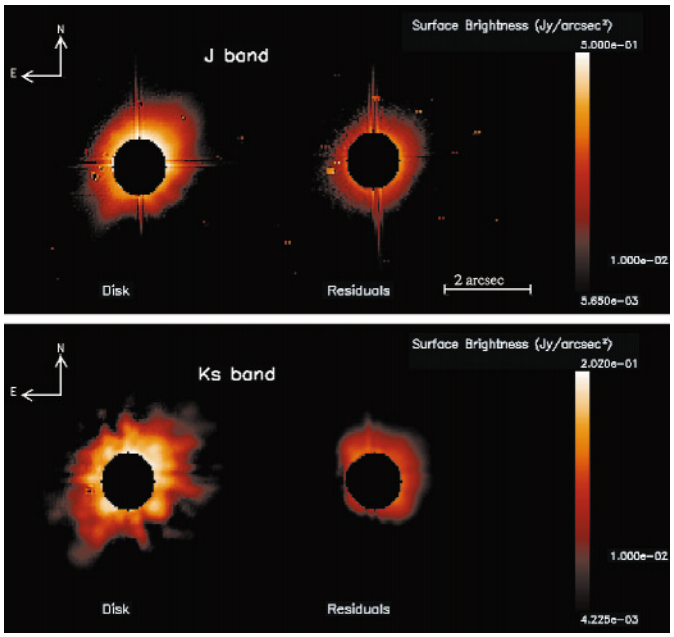

Fig. 1. Upper left: the disk seen in the J band, North is to the top, East to the left. The pixel scale is 0.035 arcsec/pixel. Upper right, the corresponding residuals obtained when applying the reduction method described in the text to two reference stars. Lower frame: same as upper frame but in the Ks filter. The "cross-like" pattern (with fingers orientations at 45,135,225, and 315 degrees) superimposed to the disk emission is produced by astigmatism residuals not corrected by the adaptive optics loop, showing that, contrarily to J band where the correction residuals are still dominated by the seeing, in Ks band under good conditions, one can reach high Strehl ratio values (i.e. system residuals dominating the uncorrected part of the seeing)

for photometric calibration. Observations of empty fields were also performed to estimate and remove the background flux which can be important in the Ks band.

3. Reduction procedure

First, standard reduction techniques were applied to the data: bias subtraction, flat-field correction. For each filter, we obtained a set of HD 100546 observations and corresponding PSFs. In spite of the use of a coronograph mask, the disk surface brightness is still dominated by the stellar emission at any distance from the star. In order to retrieve the disk image, one has to remove numerically the starlight wings. The rough substraction of a scaled PSF to HD 100546 images gives poor results because of slight shifts in position on the array between the reference and the object, uncertainties on the fluxes (given by the literature), and a residual background (ADONIS bench emission, different airmasses). We developed a specific method to get an optimum subtraction. For each couple of HD 100546 image (Obj) and corresponding Psf, we have to find 3 parameters: a shift (δx,δy) between the two images, a scaling factor R, and a residual background Bg. These parameters are estimated by minimizing the following error functional:

$$J = \sum |\text{Obj} - S(\text{Psf}/R, \delta x, \delta y) - Bg| \quad (1)$$

where the S function stands for image shift. The sum is performed on a set of pixels (typically 1000) located in a region of the images where no disk emission is expected, and from which non accurate ones are excluded (bad pixels, pixels belonging to area contaminated by diffracted light from the coronograph support). The functional minimum is found using a 0-order minimization algorithm called Powell method (Press 1996). The method was first checked on simulated data whose input parameters (shifts, scaling factor) were recovered with an accuracy better than 5%. In order to evaluate the errors in the subtraction process, test the stability of the PSF, and make sure that the disk obtained is not an artifact created by the process, the same substraction process was applied to the two different PSFs. Fig. 1 shows the resulting images in the J and Ks filters of the disk and the corresponding residuals between the two reference stars. The position of the star under the mask, and therefore the disk center is also carefully determined in this procedure thanks to offset observations (out of the coronograph mask) of the reference stars and the object.

4. Results

Since the dataset in J band is more accurate (because of a larger integration time, better observing conditions, and a better sensitivity of the whole system) than in Ks band, the geometrical parameters and the disk model are based on the J band image. We checked in a second step that the results are compatible with the Ks band data.

4.1. Disk geometrical parameters

Given a disk inclination with respect to the line of sight which is $\approx 45^\circ$, we expect to observe some deviations from the perfect ellipse case. Indeed, particles relatively large with respect to the wavelength produce non-isotropic scattering. One simple way to reduce this effect is to symmetrize the disk i.e. construct an isotropic-like virtual disk by averaging the original disk image and its symmetrical image with respect to the major axis. Best ellipse fitting on this symmetrized images gives the following results:

- disk position angle on the sky of 37 ± 5 degrees with respect to east direction.
- ellipse major to minor axis ratio of 1.2 implying a disk inclination of 50 ± 5 degrees with respect to the line of sight (or from the edge-on case).
- disk extension: ≈ 2.0 arcsec from the star corresponding to a distance to the star around 200 AU (assuming a distance to the Earth of 103 parsecs (van den Ancker et al. 1998) and a limiting sensitivity of 5 mJy/arcsec^2.

4.2. Photometry

Using the stars HD 101713 (B9V) and HD 97218 (G8) as references whose V magnitude is known and using appropriate V-J and V-Ks color indices, we derived the following photometry for the disk in J and Ks band: a disk flux in J band of

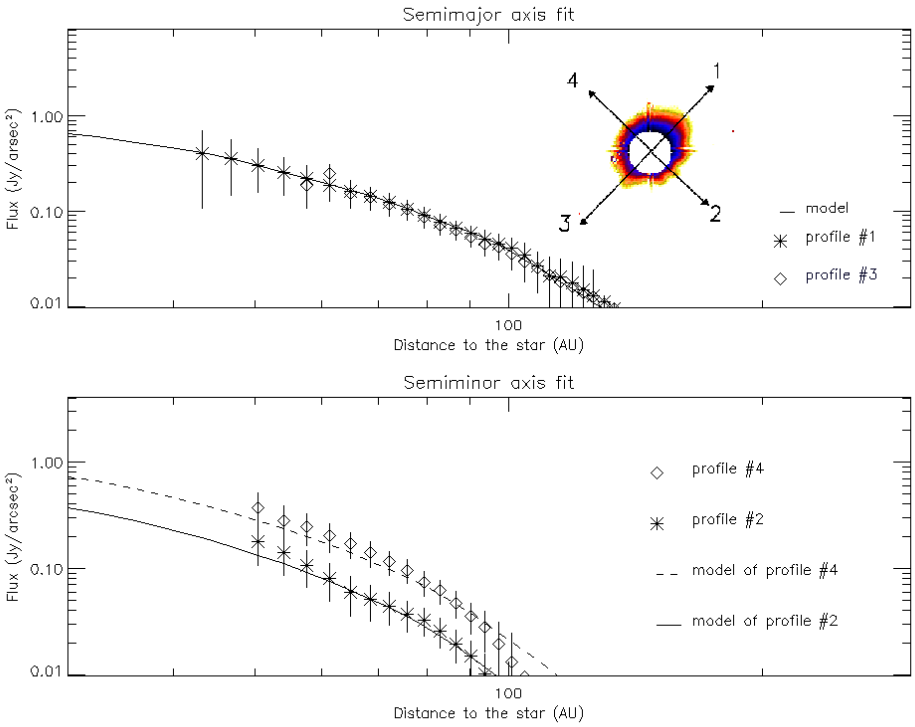

Fig. 2. Fit of the data profiles. Upper plot, full lines: the modeled profiles, stars and diamonds represent the data profiles 1 and 3 defined on the disk image inserted. Lower plot, dashed line: model of profile 4 (dominant forward scattering), plain line: model of profile 2. As seen on the lower plot, the scattering asymmetry is well reproduced by an anisotropic phase function (Henyey-Greenstein, see the text) with $g = 0.2$, corresponding to a particle size around 0.1 μm.

0.32 ± 0.06 Jy outside the coronograph mask and a maximum surface brightness of 0.5 ± 0.1 Jy/arcsec^2. From images of HD 100546 and corresponding reference star images (HD 101713 and HD97218) obtained when shifting the targets outside of the mask, we can deduce a total of scattered flux in the J band around 1 Jy; note that we get also a disk-shaped emission when removing a scaled reference to the HD 100546 image obtained outside the mask, but its signal to noise is very low. This result is compatible with the infrared excess computed considering a Kurucz model of the star (B9V spectral type). Consequently, the disk flux outside the coronograph mask represents roughly 30% of the total disk emission.

In the Ks band, we find an emission of 0.25 ± 0.1 Jy outside the coronograph mask and a maximum surface brightness of 0.25 ± 0.1 Jy/arcsec^2

4.3. Model and observation fit

In order to derive physical parameters of the disk, we built a numerical model of starlight scattering by an optically thin disk made of dust particles. Assuming that no multiple scattering is occurring in the disk, and since the exact physical properties of the particles are poorly known (composition, shape, size distribution), we chose to use a global, single-parameter, scattering phase function. The most practical one, although not realistic, is the Henyey-Greenstein phase function (Henyey & Greenstein 1941). The disk is assumed to be seen with an inclination derived above, and to have a proper thickness similar to the one of β Pic parameterized following Artymowicz et al. 1989. The disk midplane density is described by a scattering area which follows a series of broken power laws. We start with a first guess deduced from the radial surface brightness, and we iterate on the parameters until we obtain a satisfactory fit along the four directions defined on Fig. 2.

4.4. Fit results

The best fit model provides the following parameters (one must keep in mind that they are model-dependent):

- The Henyey-Greenstein phase function parameter found is $g = 0.2$ corresponding to dominant spherical particles with size around 0.1 micron.
- A radial normal optical thickness fitted by a series of broken power laws whose exponents are: 0.6 in the range [10,45]AU, -0.4 in the range [45,70]AU, -1.35 in the range [70,100]AU, -5 outwards from 100 AU, see Fig. 3.
- An exponentially decreasing vertical profile, and an opening angle around 0.1 radian.
- A total scattering area of 10^{29} cm^2 and a dust mass of 0.02 $M_\oplus$.
- An approximate disk surface density at maximum around 3×10^{14} particles/m^2 assuming single-sized particles of 0.1 μm, or an equivalent maximum scattering area of the order of the unity/m^2.

5. Discussion

The radial surface brightness distribution shows that the disk density peaks at a distance of 40 AU from the star corresponding to the edge of the planetary zone in our solar system. The normal optical thickness found is more than 100 times larger than in the case of the β Pic disk. Simultaneously, the presence of sub-micronic particles sizes, well below the radiation pressure cut-off in sizes, suggests that huge quantities of very small

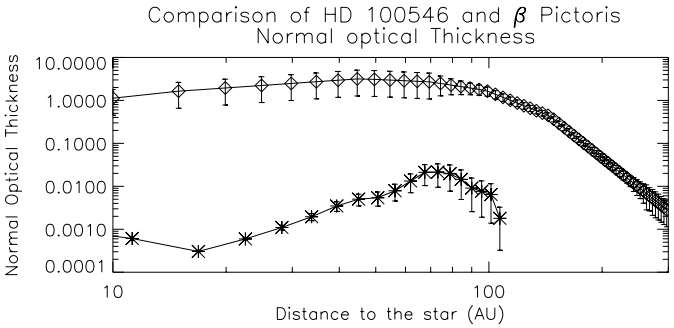

Fig. 3. The normal optical thickness of the disk deduced from model fitting of the data (diamonds). We have overplotted (stars) the normal optical thickness found in the case of the disk around β Pictoris (Pantin, Lagage & Artymowicz 1998)

particles are produced continuously by evaporation or collisions of planetesimals. We are probably witnessing a analogue of the young Kuiper belt with planetesimals undergoing violent agitation. If the dust particles are the result of collisions, a high rate is required to produce the observed disk. This implies that gravitational perturbations occur frequently in this disk, maybe because of giant planets. If the disk is replenished by planetesimal evaporation as suggested by Lecavelier des Etangs (1998) in the case of the β Pic disk, 10^9 planetesimals (40 km size) whose orbits were recently perturbed by planet migration are required to maintain the disk. Some of them which orbits are gravitationally perturbed might be the origin of the casual redshifted absorption profiles observed in some of the spectra of HD 100546 (Grady et al. 1997), a phenomenon highly similar to what is observed in the system of β Pictoris (Lagrange-Henry et al. 1987, Beust et al. 1996).

6. Conclusion

Thanks to coronograph adaptive optics observations we could detect the disk surrounding the PMS star HD 100546. This detection of a disk which is believed to represent a class of precursors to β Pic-like disks adds a new clue in the understanding of the formation and evolution of these debris disks. Other imaging observations of disks at various stage of evolution are necessary to sketch more closely the possible scenario of such a disk creation and evolution. This should be achieved by next generation instruments such as the VLT/NAOS (adaptive optics) and VLT/VISIR (mid-infrared) instruments or the NGST.

Acknowledgements. We would like to express our warm gratitude to the persons who helped in achieving these observations: D. Le Mignant, F. Marchis, O. Marco, V. Meriño, E. Wenderoth, and the whole 3.6m team.

References

Augereau, J. C., Lagrange, A. M., Mouillet, D., Papaloizou, J. C. B. & Grorod, P. A., 1999, A&A, 348, 557
Artymowicz, P., Burrows, C., & Paresce, F., 1989, ApJ, 337, 494
Augereau, J. C., Lagrange, A. M., Mouillet, D. & Ménard, F., 1999, A&A, 350, 51
Aumann, H. H. et al., 1984, ApJ, 278, L23
Beust, H., Lagrange, A.M., PLazy, F., & Mouillet, D., 1996, A&A, 310, 181
Beuzit, J.-L., Mouillet, D., Lagrange, A.-M. & Paufique, J., 1997, A&AS, 125, 175–182
Jayawardhana, R. et al., 1998, ApJ, 503, L79
Koerner, D. W., Ressler, M. E., Werner, M. W. & Backman, D. E., 1998, ApJ, 503, L83
Henyey, L.G. & Greenstein, J.L., 1941, ApJ, 93, 70
Lagage, P. O. & Pantin, E., 1994, Nature, 369, 628
Lagrange-Henry, A.M., Ferlet, R., & Vidal-Madjar, A., 1987, A&A, 173, 289
Lecavelier Des Etangs, A., 1998, A&A, 337, 501
Malfait, K., Bogaert, E. & Waelkens, C., 1998a, A&A, 331, 211
Malfait, K., Waelkens, C., Waters, L. B. F. M., Vandenbussche, B., Huygen, E. & de Graauw, M. S., 1998b, A&A, 332, L25
Pantin, E., Lagage, P. O. & Artymowicz, P., 1997, A&A, 327, 1123
Plets, H. & Vynckier, C., 1999, A&A, 343, 496
Press, W. H., 1996, in *Numerical Recipes*, Cambridge University Press
Schneider, G. et al., 1999, ApJ, 513, L127
Smith, B. A. & Terrile, R. J., 1984, Science, 226, 1421
van den Ancker, M. E.,de Winter, D. & Tjin A Djie, H. R. E., 1998, A&A, 330, 145
Waelkens et al., 1996, A&A, 315, L245
Weinberger, A. J. et al., 1999, ApJ, 525, L53